ISSN: 0256-307X

中国物理快报
Chinese Physics Letters

Volume 29 Number 8 August 2012

A Series Journal of the Chinese Physical Society
Distributed by IOP Publishing

Online: http://iopscience.iop.org/cpl
http://cpl.iphy.ac.cn

CHINESE PHYSICAL SOCIETY
IOP Publishing

CHIN. PHYS. LETT. Vol. 29, No. 8 (2012) 089601

Cross-Shock Electrostatic Potential and Ion Reflection in Quasi-Parallel Supercritical Collisionless Shocks *

SU Yan-Qing(苏彦青)[1], LU Quan-Ming(陆全明)[1,2]**

[1] CAS Key Laboratory of Basic Plasma Physics, Department of Geophysics and Planetary Science, University of Science and Technology of China, Hefei 230026

[2] State Key Laboratory of Space Weather, Chinese Academy of Sciences, Beijing 100190

(Received 9 March 2012)

The time evolution of the cross-shock electrostatic potential jump during one specific high Mach number quasi-parallel shock reformation cycle is examined via a 1D hybrid simulation. It is shown that when the average value of the electrostatic potential jump is low, its instant value can be large so that the shock is in a favorable profile to directly reflect the incident ions. Our simulation also suggests that, for the ones that finally become injected ions (which can be further accelerated by diffusive shock acceleration mechanism), the first step of their reflections should be mainly attributed to the electrostatic potential jump, instead of the magnetic force, as stated in some previous studies.

PACS: 96.50.Fm, 96.50.Ry DOI: 10.1088/0256-307X/29/8/089601

In space and astrophysical plasma, collisionless shocks are of much concern not only in the particle heating, but also in the explanation of high energy particles. The theory of diffusive shock acceleration (DSA) has been very successful in explaining the high energy tail of the cosmic ray spectrum associated with shocks.[1−11] At a quasi-parallel shock ($\theta_{Bn} < 45^\circ$ with θ_{Bn} being the shock angle between the upstream magnetic field and the shock's normal direction), where the upstream waves and downstream waves are rich, DSA works more efficiently because ions are more easily scattered back and forth to cross the shock many times, gaining very high energies. In DSA mechanism, an injection problem around how a small fraction of seed particles are extracted from the thermal background plasma to generate superthermal ions for a further diffusive acceleration process has not been well addressed.[12−14]

Since initially performed by Kan and Swift[15] and Quest,[16] the hybrid simulation has been considered a powerful tool to investigate the origin of diffuse superthermal ions as well as the details of the quasi-parallel shock structure. Specifically by this method, Burgess[17] found that the high Mach number quasi-parallel shocks exhibit a cyclic behaviour and reform periodically, which has been confirmed by numerous later researches. According to previous observations and simulations, ion reflection is very common in quasi-parallel supercritical collisionless shocks.[18−20] Ions can be periodically reflected by the shock front during the shock reformation, which seems to be initiated by the coherently reflected process.[21,22]

In this work, self-consistent 1D hybrid simulations (ions are treated kinetically, while the electrons are treated to be massless, adiabatic fluid) of high Mach number quasi-parallel shock were performed to study the ion reflection and electrostatic potential jump. The results suggest that the electrostatic potential jump plays an important role in extracting the seed particle from the thermal background plasma.

Initially, the magnetic field lied in the x–y plane and the shock was generated in the downstream system by the method of a rigid wall that was located at the right side of the simulation box. An upstream ion flow with a bulk velocity of $4.5v_A$ (Alfven velocity) continued to be injected from left to right; then when reaching the right wall located at the right boundary of the simulation area, the ions were secularly reflected. In this way, a shock was generated, and proceeded to the left. Fixed and free escape boundary conditions were employed in our simulation, with its simulation size of $1800c/\omega_{pi}$ (the grid size is $\Delta x{\sim}0.3c/\omega_{pi}$) and the time step $\Delta t{\sim}0.02\Omega_i^{-1}$. There are 200 particles (pure protons) in each cell, where the Alfven Mach number $M_A = 5.5$, upstream shock angle $\theta_{Bn} = 30^\circ$, upstream ion beta $\beta_i = 0.1$ and electron beta $\beta_e = 0.5$. In order to better analyze the results, several flags were added to every particle to restore their histories of the interactions with the shock at the beginning of the simulations.

Figure 1 shows the overall evolution of the total magnetic field strength B from $\Omega_i t = 90$ to $\Omega_i t = 150$

*Supported by the National Natural Science Foundation of China under Grant Nos 40931053, 41174114 and 41121003, the Ocean Public Welfare Scientific Research Project, State Oceanic Administration People's Republic of China (No 201005017), and the Fundamental Research Funds for the Central Universities (WK2080000010).

**To whom correspondence should be addressed. Email: qmlu@ustc.edu.cn

between $x = 1500c/\omega_{pi}$ and $x = 1800c/\omega_{pi}$. In this time interval, the shock propagates from right to left with an average velocity of $1.0v_A$. In the upstream side, the ultra-low frequency (ULF) wave excited by the backstreaming ions has an upstream directed group velocity; it is then brought back into the shock by the upstream incident flow. When running into the shock, the ULF wave can grow its amplitude and form a shocklet; then this shocklet merges with the local shock front, facilitating the formation of a new shock front. In our simulation, the shock front repeats itself on the time scale of tens of upstream ion gyrating periods.

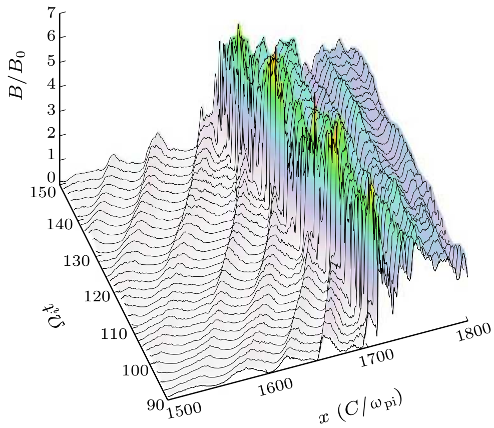

Fig. 1. Surface plot of the total magnetic field B with different colors representing different magnitudes from $\Omega_i t = 90$ to $\Omega_i t = 150$. The displayed area is cut between $x = 1500\lambda_i$ and $x = 1800\lambda_i$.

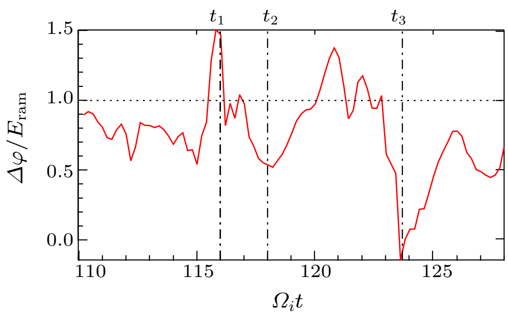

Fig. 2. The evolution of the electrostatic potential jump $\Delta\varphi$ in units of the shock ram energy $E_{\rm ram}$ from $\Omega_i t = 110$ to $\Omega_i t = 125$. The three dot-dashed lines indicate three different time points, with $\Omega_i t_1 = 116$, $\Omega_i t_2 = 118$, and $\Omega_i t_3 = 123.7$.

The electrostatic potential jump in the normal incident frame (NIF) during the time period from $\Omega_i t = 110$ to $\Omega_i t = 128$ was calculated with the definition $\boldsymbol{E} = -\nabla\varphi$, and its evolution $\Delta\varphi$ is plotted in Fig. 2, in units of the shock ram energy $E_{\rm ram}$ (the incident flow energy $\frac{1}{2}mV_i^2$ in shock frame). It is found that the average $\Delta\varphi$ is around 80% of $E_{\rm ram}$. Nevertheless, during one reformation cycle, the value of $\Delta\varphi$ varies with time: when the incident ions confront the shock at, e.g., t_1, it is difficult for the particle to transmit to the downstream due to the large electrostatic potential gradient force; while at times like t_2 or t_3, $\Delta\varphi$ is very small or nearly zero, so that the incident ions can transmit to the downstream side of the shock more freely.

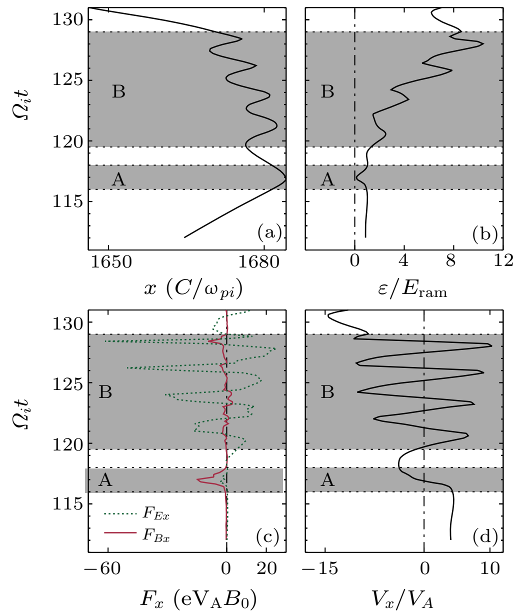

Fig. 3. The four panels indicate the time evolution of the position in the normal direction x of the particle (a), the total energy gain $\varepsilon = v^2/2$ in shock rest frame in units of the shock ram energy (b), the x component force with its two components F_{Ex} and F_{Bx}, with each obtained from the electric field and magnetic field (c), and x component velocity v_x (d). The shadowed regions A and B are the initial reflection period and the trap-acceleration process, respectively. This particle first encounters the shock at $\Omega_i t = 116$ indicated by t_1 in Fig. 2, corresponding to the bottom boundary of the region A here.

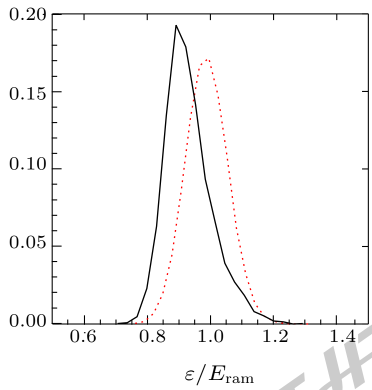

Fig. 4. Plots of the energy of ions with respect to the shock ram energy in shock rest frame. The solid curve is the energy distribution of the seed particles that are finally to be injected; the energy distribution of the back ground ions in the upstream flow is also provided for reference (dotted curve). Note that these two distributions are normalized respectively.

The injected ions, which can finally escape to the upstream, are discussed in the following. For a detailed analysis, all the particles reflected by the shock during the period between $\Omega_i t = 110$ to $\Omega_i t = 128$ are studied (Fig. 2). The evolutions of the relative quantities of a typical injected ion including position x, energy ε, x-component force read $F_x = qE_x + q(\boldsymbol{v} \times \boldsymbol{B})_x = F_{Ex} + F_{Bx}$, x-component velocity v_x (also the normal direction velocity), are plotted in Fig. 3. After examining all the injected ions, we divide the injection process into two steps: reflection process and acceleration process, corresponding to the two shaded areas A and B, respectively. Only step A is discussed in this study, while step B will be investigated in our successive papers. During the time period shown in Fig. 3, we should bear in mind that the shock was propagating to the left side of the simulation area. Before step A, the particle was streaming to the shock in the upstream. When encountering the shock for the first time at $\Omega_i t = 116$ indicated by the base line of region A, the particle started to decelerate to $\varepsilon = 0$ (Fig. 3(b)) and $v_x = 0$ (Fig. 3(d)) due to the large negative x-component electric force F_{Ex} (Fig. 3(c)). The particle was further accelerated to have a large negative x-component velocity (see the upper line of region A in Fig. 3(d)). Once it obtains the large negative v_x, the particle will go to the upstream, however, not very far away from the shock, and it immediately becomes trapped and accelerated by the shock in step B (Figs. 3(a) and 3(b)). Finally, after step B, it can escape from the trap of the shock and stream far upstream (Figs. 3(a) and 3(d)). Comparing the above steps, we find that F_x was mainly contributed by the electric force F_{Ex} in step A, while totally by the $\boldsymbol{v} \times \boldsymbol{B}$ term F_{Bx} during step B. Other injected particles during this time period share the same characteristics: when first encountering the shock at times like t_1, they see a very large electrostatic potential gradient force at the shock, and are easily reflected back to the upstream (most of them were nearly secularly reflected). On the contrary, usually, the directly transmitted ions entered the shock at time like t_2 in Fig. 2, when the shock's electrostatic potential jump was low, so that there were barely barriers for the incident ions to get transmitted.

Previous studies showed that the cross-shock's electrostatic potential gradient force is less important than the magnetic field in reflecting incident ions in quasi-parallel shocks.[8] However, our simulation results suggest that all the obvious coherently reflected ion beams happened when there was a large $\Delta\varphi$ near the shock front, while the magnetic force was low. Note that after the first reflection, the magnetic force can begin to play a more important role.

At the end of the simulation, all the ions that had once been injected were carefully selected based on their flags. Then we checked their initial energies when they were still in the upstream as the seed particles, before interacting with the shock. The initial energy distribution of these injected ions (solid curve) and the background upstream ions (dotted curve), which are normalized independently, are plotted in Fig. 4. The peak of the seed particles energy distribution is around $0.9E_{\rm ram}$, which is relatively low compared to the full distribution of the whole upstream incident flow. It is a reasonable result because compared with the higher energy particles, the particles of lower energy can be more easily reflected when confronted with the same cross-shock electrostatic potential. The results shown by Fig. 4 are somewhat different from previous studies. This work's results are in agreement with Scholer *et al.*,[20] i.e., instead of from the core of the incident flow, seed particles originate from the thermal part of the incident flow. Further, the seed particles in our simulation are mainly of lower velocity, which is reasonable when the impact of the variation of the electrostatic potential jump during a shock reformation cycle is taken into account.

The electrostatic potential jump has long been ignored in reflecting upstream ions in quasi-parallel shocks, especially in building injection models. According to previous studies, the electrostatic potential jump can only reach a value that is no more than 30% of the energy of the incident flow when the Mach number is high.[23,24] In these works, they assume that the shock's structure is steady (not time varying). Although some of these results were obtained from the De-Hoffman Teller frame, in which the motional electric field would vanish, it is still reasonable to include the influence of the shock reformation process in calculating the electrostatic potential jump. Without the consideration of the reformation process, one could easily underestimate the instant value of the electrostatic potential jump. Also, a single spacecraft can not resolve time and space, thus the electric field strength measured is often an instant value. As in our simulation in NIF frame, although on average, the electrostatic potential jump was low, it can reach a very large value during the reformation cycle. The instant electrostatic potential jump may reach or even exceed the shock's ram energy. Also, our results show that the magnetic force alone cannot reflect the incident flow without the large electrostatic potential gradient force. For instance, at t_2 or t_3 in Fig. 2, although the local magnetic field is very large, there are barely any incident ions reflected, because there is a very low (nearly zero) electrostatic potential jump. As a result of the influence of the electrostatic potential jump on the ion reflection process, the seed particles are mainly from the lower velocity part of the upstream incident flow ions.

To some extent, it is the time when the incident ion encounters the shock that really determines the fate of the ion. Whether the ion will penetrate to the downstream region or be reflected to the upstream region is subject to the instant electrostatic potential jump of the shock front. Thus, whether an ion can be a seed particle to be injected is also influenced by the instant electrostatic potential jump.

References

[1] Blandford R D and Ostriker J P 1978 *Astrophys. J.* **221** L29

[2] Axford W I, Leer E and Skadron G 1977 *Proc. 15th Int. Cosmic Ray Conference* (Plovdiv, Bulgaria 13–26 August 1977) vol 11 p 132

[3] Bell A R 1978 *Mon. Not. R. Astron. Soc.* **182** 147

[4] Bell A R 1978 *Mon. Not. R. Astron. Soc.* **182** 443

[5] Lee M A 1983 *J. Geophys. Res.* **88** 6109

[6] Blandford R and Eichler D 1987 *Phys. Rep.* **154** 1

[7] Webb G M, Zank G P, Ko C M and Donohue D J 1995 *Astrophys. J.* **29** 453

[8] Malkov M A and Drury L O 2001 *Rep. Prog. Phys.* **64** 429

[9] Li G, Zank G P and Rice W K M 2003 *J. Geophys. Res.* **108** 1082

[10] Giacalone J 2004 *Astrophys. J.* **609** 452

[11] Zank G P, Li G, Florinski V, Hu Q, Lario D and Smith C W 2006 *J. Geophys. Res.* **111** A06108

[12] Hussain S 2012 *Chin. Phys. Lett.* **29** 065202

[13] Zou X, Liu H P, Qiu M H and Sun X H 2011 *Chin. Phys. Lett.* **28** 125201

[14] Qureshi M N S, Shi J K, Torkar K and Liu Z X 2011 *Chin. Phys. Lett.* **28** 025204

[15] Kan J R and Swift D W 1983 *J. Geophys. Res.* **88** 6919

[16] Quest K B 1988 *J. Geophys. Res.* **93** 9649

[17] Burgess D 1989 *Geophys. Res. Lett.* **16** 345

[18] Gosling J T, Thomsen M F, Bame S J and Russell C T 1989 *J. Geophys. Res.* **94** 10027

[19] Onsager T G, Thomsen M F, Gosling J T, Bame S J and Russell C T 1990 *J. Geophys. Res.* **95** 2261

[20] Scholer M and Terasawa T 1990 *Geophys. Res. Lett.* **17** 119

[21] Li B, Chen Y J and Li X 2011 *Chin. Phys. Lett.* **28** 059601

[22] Singh M, Singh L P and Husain A 2011 *Chin. Phys. Lett.* **28** 094701

[23] Mandt M E and Kan J R 1991 *J. Geophys. Res.* **96** 21391

[24] Schwartz S J, Thomsen M F, Bame S J and Stansberry J 1988 *J. Geophys. Res.* **93** 12923

Chinese Physics Letters

Volume 29 Number 8 August 2012

ATOMIC AND MOLECULAR PHYSICS

FUNDAMENTAL AREAS OF PHENOMENOLOGY(INCLUDING APPLICATIONS)

CROSS-DISCIPLINARY PHYSICS AND RELATED AREAS OF SCIENCE AND TECHNOLOGY

GEOPHYSICS, ASTRONOMY, AND ASTROPHYSICS